

UC Davis

UC Davis Previously Published Works

Title

R2R3 MYB-dependent auxin signalling regulates trichome formation, and increased trichome density confers spider mite tolerance on tomato

Permalink

<https://escholarship.org/uc/item/27v1c7kg>

Journal

Plant Biotechnology Journal, 19(1)

ISSN

1467-7644

Authors

Yuan, Yujin

Xu, Xin

Luo, Yingqing

et al.

Publication Date




2021

DOI

10.1111/pbi.13448

Peer reviewed

R2R3 MYB-dependent auxin signalling regulates trichome formation, and increased trichome density confers spider mite tolerance on tomato

Yujin Yuan^{1,2,3,†} , Xin Xu^{1,2,†}, Yingqing Luo^{1,2}, Zehao Gong^{1,2}, Xiaowei Hu^{1,2}, Mengbo Wu^{1,2}, Yudong Liu^{1,2}, Fang Yan^{1,2}, Xiaolan Zhang^{1,2}, Wenfa Zhang^{1,2}, Yuwei Tang^{1,2}, Bihong Feng⁴, Zhengguo Li^{1,2} , Cai-Zhong Jiang^{3,5} and Wei Deng^{1,2,*} 

¹Key Laboratory of Plant Hormones and Development Regulation of Chongqing, School of Life Sciences, Chongqing University, Chongqing, China

²Center of Plant Functional Genomics, Institute of Advanced Interdisciplinary Studies, Chongqing University, Chongqing, China

³Department of Plant Sciences, University of California, Davis, CA, USA

⁴College of Agriculture, Guangxi University, Nanning, China

⁵Crops Pathology and Genetics Research Unit, United States Department of Agriculture, Agricultural Research Service, Davis, CA, USA

Received 9 March 2020;

revised 22 June 2020;

accepted 6 July 2020.

*Correspondence (Tel +86 18623127580;

fax +86 23 65678902; email

dengwei1977@cqu.edu.cn)

[†]These two authors equally contribute to this work and are considered as co-first authors.

Summary

Unicellular and multicellular tomato trichomes function as mechanical and chemical barriers against herbivores. Auxin treatment increased the formation of II, V and VI type trichomes in tomato leaves. The auxin response factor gene *SIARF4*, which was highly expressed in II, V and VI type trichomes, positively regulated the auxin-induced formation of II, V and VI type trichomes in the tomato leaves. *SIARF4* overexpression plants with high densities of these trichomes exhibited tolerance to spider mites. Two R2R3 MYB genes, *SITHM1* and *SIMYB52*, were directly targeted and inhibited by *SIARF4*. *SITHM1* was specifically expressed in II and VI type trichomes and negatively regulated the auxin-induced formation of II and VI type trichomes in the tomato leaves. *SITHM1* down-regulation plants with high densities of II and VI type trichomes also showed tolerance to spider mites. *SIMYB52* was specifically expressed in V type trichomes and negatively regulated the auxin-induced formation of V type trichome in the tomato leaves. The regulation of *SIARF4* on the formation of II, V and VI type trichomes depended on *SITHM1* and *SIMYB52*, which directly targeted cyclin gene *SICycB2* and increased its expression. In conclusion, our data indicates that the R2R3 MYB-dependent auxin signalling pathway regulates the formation of II, V and VI type trichomes in tomato leaves. Our study provides an effective method for improving the tolerance of tomato to spider mites.

Keywords: trichome, auxin response factor, MYB, transcription factor, tomato.

Introduction

Pests have threatened crop yield since the commencement of plant domestication. At present, pest invasion ruins approximately 13% of crop production globally (Hamza *et al.*, 2018). Plants tactically developed response mechanisms against pest attacks. They developed mechanical and chemical barriers in the form of trichomes. Differentiated epidermal cells from leaves, stems and floral organs produce plant trichomes, which can be glandular or nonglandular, unicellular or multicellular, and branched or unbranched (Yang and Ye, 2013).

Trichomes are nonglandular, unicellular and branched in *Arabidopsis*. Trichome formation passes through three stages: cellular determination, specification and morphogenesis of epidermal cell (Yang and Ye, 2013). A trimeric transcription factor (TF) complex formed by R2R3 MYB, WD40 repeat and basic helix–loop–helix (bHLH) proteins positively regulates trichome formation (Ishida *et al.*, 2008). The WD40–bHLH–MYB complex directly induces the expression of *GLABRA2* and cell cycle-related *SIAMESE* (Morohashi and Grotewold, 2009). R3 MYBs compete with R2R3 MYBs and form a repressor complex that inhibits trichome formation (Wang *et al.*, 2007).

Tomato has several types of trichomes: II, III, V and VIII type, which are nonglandular trichomes, and I, IV, VI and VII type, which are multicellular glandular trichomes (Glas *et al.*, 2012). Glandular trichomes produce volatile organic compounds (VOCs) to repel or eradicate pests (Turlings *et al.*, 1995). Tomato's jasmonic acid (JA) signal transduction *CO11* regulates VI type glandular trichome formation (Li *et al.*, 2004). Tomato Woolly (*Wo*), a homeodomain-leucine zipper (HD-Zip) TF, interacts with B-type cyclin *SICycB2* protein, which are essential for the formation of type I trichomes in tomato (Yang *et al.*, 2011; Yang and Ye, 2013). The overexpression of *Wo* in potato and tobacco can promote the production of multicellular trichomes and increase tolerance to aphids (Yang *et al.*, 2015). A single cysteine2–histidine2 (C2H2) zinc-finger TF *Hair* (*H*) gene, which interacts with *Wo*, regulates the formation of type I multicellular trichomes (Chang *et al.*, 2018). *SIMYC1*, a basic bHLH TF, plays important roles in the formation of VI type glandular trichomes and terpene biosynthesis in tomato glandular cells (Xu *et al.*, 2018). The overexpression of the MYB gene *GLABROUS1* involved in unicellular trichome formation in *Arabidopsis* does not affect multicellular trichome formation in *Nicotiana*, a Solanaceae species (Payne *et al.*, 1999). The formation of

multicellular trichomes in *Solanaceae* may be controlled by a pathway that is different from that of unicellular trichomes in *Arabidopsis* (Payne *et al.*, 1999). However, the regulatory mechanism involved in nonglandular and glandular trichome formation in *Solanaceae* is rarely studied in tomato.

Auxin plays important roles in several physiological processes in plants. Short-lived auxin/indole acetic acid (Aux/IAA) proteins and auxin response factors (ARFs) are involved in auxin-dependent transcriptional regulation. At low auxin levels, Aux/IAA proteins interact with ARFs to repress ARF transcription activity by recruiting the co-repressor TOPLESS (Szemenyei *et al.*, 2008). At high auxin levels, Aux/IAs bind to the SCF^{TIR1/AFB} complexes degraded by the 26S proteasomes and release ARFs, which regulate the transcription of auxin response genes (Wang and Estelle, 2014). ARFs act as the transcriptional repressors or activators of auxin-responsive genes (Guilfoyle and Hagen, 2012; Ren *et al.*, 2011). Most ARF proteins have an N-terminal DNA-binding domain (B3) for the regulation of the transcription of auxin response genes, a middle region as an activation or repression domain, and a C-terminal dimerization domain (Aux/IAA) for the formation of homo- or heterodimers (Krogan and Berleth, 2012; Zouine *et al.*, 2014). ARFs play important roles in various plant developmental processes (Ckurshumova *et al.*, 2014). *SIARF4* is a repressor of auxin response and regulates the accumulation of chlorophyll and starch in tomato fruits (Sagar *et al.*, 2013).

The tomato Aux/IAA family gene *SIIAA15* is involved in the formation of glandular and nonglandular trichomes (Deng *et al.*, 2012). However, the mechanism of auxin-mediated transcriptional regulation of trichome formation in tomato still needs to be elucidated. In this study, auxin treatment increased the densities of II, V and VI type trichomes in tomato. *SIARF4* positively regulated the auxin-induced formation of II, V and VI type trichomes, and the regulation was dependent on R2R3 MYB TFs *SITHM1* and *SIMYB52*. Transgenic plants with high densities of trichomes because of the overexpression of *SIARF4* or down-regulation of *SITHM1* increased trichome density and conferred spider mite tolerance. Overall, our results showed that an auxin-mediated regulatory pathway regulated formation of nonglandular and glandular trichomes and provided an effective method for improving the tolerance of tomato plants to spider mites.

Results

Auxin treatment induced the formation of II, V and VI type trichomes in leaves

Different type of trichomes was first identified by scanning electron microscopy (SEM) on the adaxial leaf surfaces of 'Micro-Tom' tomato cultivar. It is clear that II, V and VI type trichomes were abundant and easily recognizable (Glas *et al.*, 2012). Therefore, II, V and VI type trichomes on the adaxial leaf surfaces were studied. The influence of auxin on tomato trichome formation was investigated by treating tomato seedlings with various concentrations of IAA (Indole acetic acid). The densities of II, V and VI type trichomes increased with IAA concentration (from 1 mg/L to 30 mg/L), and the most obvious effects on trichome densities was 30 mg/L IAA (Figure 1a). Thus, this concentration was used in subsequent analysis. Given that trichomes are initiated from the epidermal pavement cells of leaves, the effects of auxin treatment on the densities of epidermal pavement cells were analysed. IAA treatment had no effect on the density of epidermal pavement cells (Figure S1). Our

result indicated that auxin induced the formation of type II, V and VI trichomes in the tomato leaves.

SIARF4 positively regulated the auxin-induced formation of II, V and VI type trichomes in the leaves

qRT-PCR was performed to assess the expression pattern of *SIARF4* (Figure S2). *SIARF4* is highly expressed in leaf trichomes. The expression pattern of *SIARF4* in leaves was further analysed by GUS staining. A transcriptional fusion was generated between *SIARF4* promoter and *GUS* gene (p*SIARF4*-GUS), and GUS staining was detected in II, V and VI type trichomes (Figures 1b, d and f). No GUS staining was detected in the trichomes of WT plants (Figures 1c, e and g). This result indicated that *SIARF4* was expressed in II, V and VI type trichomes in tomato leaves.

The role of *SIARF4* in trichome formation was elucidated using transgenic technology. The expression level of *SIARF4* decreased in the RNAi-*SIARF4* lines and increased in the OE-*SIARF4* lines (Figure 1h). Without IAA treatment, the OE-*SIARF4* lines displayed increases in the densities of II, V and VI type trichomes in the leaves, whereas the RNAi lines exhibited decreases in the densities of II, V and VI type trichomes compared with WT plants (Figures 1i and j). The OE-*SIARF4* lines displayed increase in the density of epidermal pavement cells in the leaves, whereas RNAi lines exhibited decreased density compared with WT plants (Figure S3). Then, the number of trichomes per epidermal cell in the OE-*SIARF4* and RNAi-*SIARF4* lines was calculated. An apparent increase in the number of trichomes per epidermal cell in the overexpressed lines and decrease in that of the RNAi lines were observed (Figure 1k), indicating that *SIARF4* positively regulated the formation of II, V and VI type trichomes. IAA treatment was performed to study the response of *SIARF4* transgenic lines to auxin. At 30 mg/L IAA concentration, the densities of II, V and VI type trichomes increased in the leaves of OE-*SIARF4*, RNAi-*SIARF4* and WT plants (Figure 1l). The trichome density ratio between IAA treatment and no-IAA treatment was calculated in studying the effect of auxin treatment on trichome formation. The ratio of OE-*SIARF4* plants was similar to that of the WT plants, but RNAi-*SIARF4* plants had lower ratio than the OE-*SIARF4* and WT plants (Figure 1m). These results indicated that the down-regulation of *SIARF4* decreases the effect of IAA treatment on the formation of II, V and VI type trichomes in tomato leaves and that the inducement of auxin on the formation of II, V and VI type trichomes is dependent on *SIARF4*. Given the fact that *SIARF4* was expressed in tomato fruits, the fruit trichome density was analysed. There was no significant difference between WT and *SIARF4* transgenic lines (Figure S4).

The function of *SIARF4* in trichome formation was validated in *Siarf4* CRISPR/Cas9 plants. The trichome density and the number of trichomes per epidermal cell were consistent with those in the RNAi-*SIARF4* plants (Figure S5), indicating *SIARF4* positively regulates the formation of II, V and VI type trichomes in tomato leaves.

Overexpression of *SIARF4* conferred spider mite tolerance to tomato

The response of *SIARF4* transgenic plants to spider mite was analysed through spider mite bioassays. Pest preference experiment was used in assessing the relative preference of herbivores for WT, OE-*SIARF4* and RNAi-*SIARF4* plants. The number of spider mites that preferred the leaves of the OE-*SIARF4* plants was lower than that of the spider mites that preferred the WT plants (Figures 2a and b). The number of spider mites that preferred the

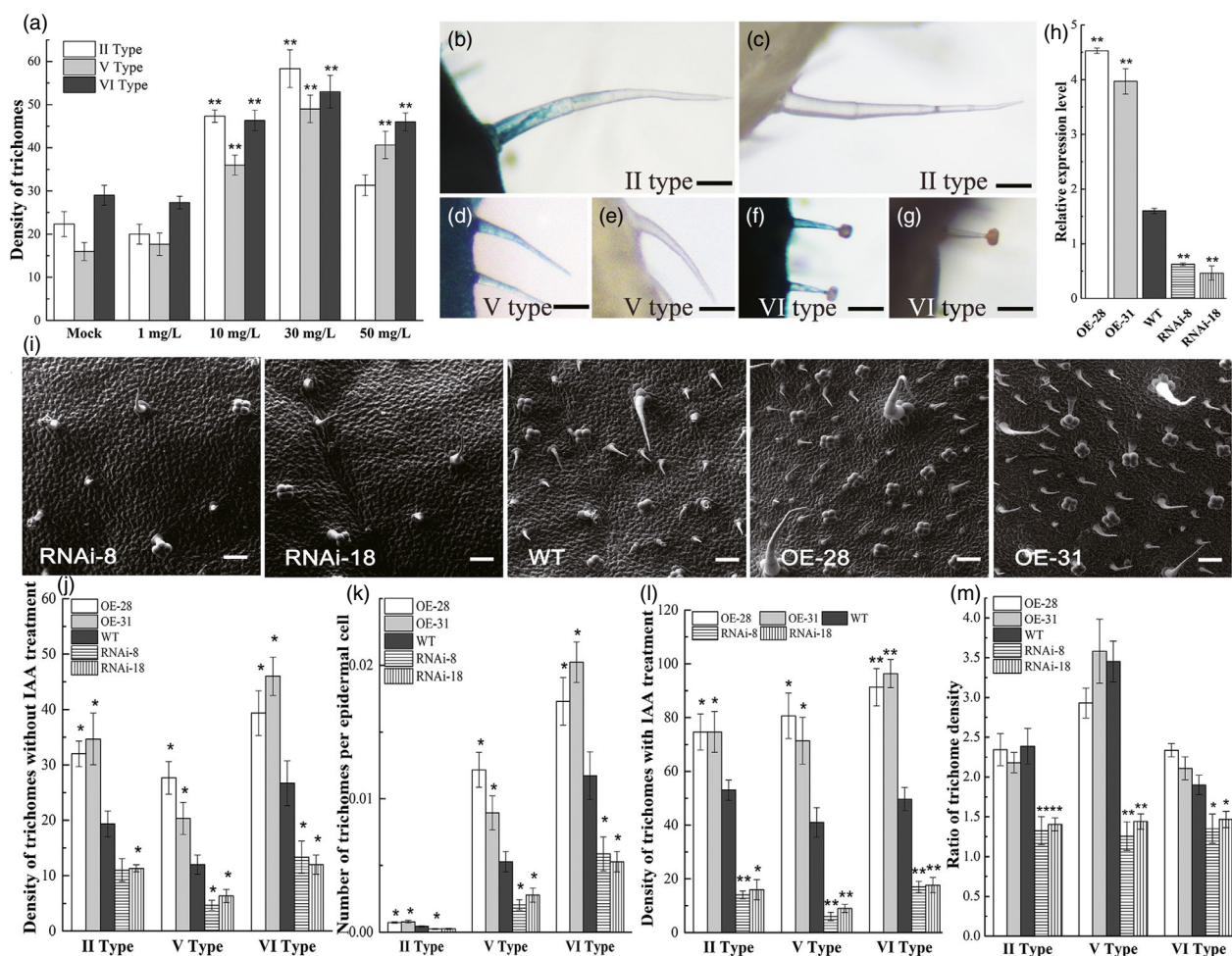


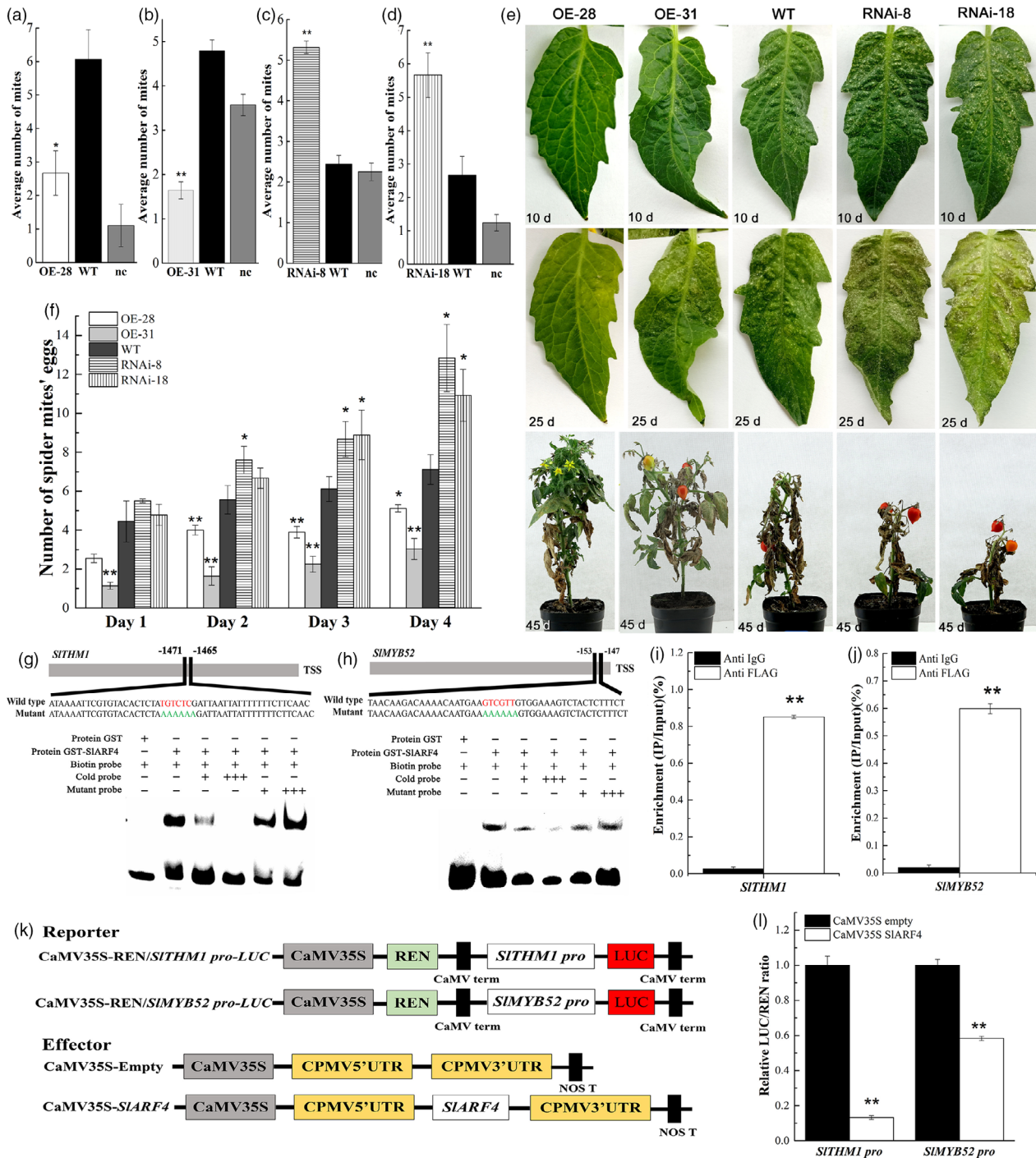
Figure 1 Trichome density with auxin treatment, expression analysis of *SIARF4* and trichome density in *SIARF4* overexpression and RNAi plants. a, Densities of II, V and VI type trichomes of tomato leaves with IAA treatment. b, d and f, Expression pattern of *SIARF4* in trichome tissues was explored by GUS reporter gene driven by the *SIARF4* promoter. Scale bars = 0.2 mm. b, II type trichome of pSIARF4-GUS lines. d, V type trichome of pSIARF4-GUS lines. f, V type trichome of pSIARF4-GUS lines. c, e and g, Gus staining of trichome tissues of WT. Scale bars = 0.2 mm. c, type II trichome of WT. e, V type trichome of WT. g, VI type trichome of WT. h, qRT-PCR analysis of *SIARF4* expression in overexpression and down-regulation lines. Each value indicates the mean \pm standard errors (SE) of four biological replicates. i, Scanning electron micrographs of the leaf surface. Scale bars = 60 μ m. j, Density analysis of II, V and VI type trichomes in the leaves of WT and *SIARF4* lines without IAA treatment. k, Number of trichomes per epidermal cell of the tomato leaves of WT and *SIARF4* lines. l, Density analysis of II, V and VI type trichomes in the leaves of WT and *SIARF4* lines with IAA treatment. m, Trichome density ratio of IAA treatment to no-IAA treatment. WT, wild-type plants; OE-28 and -31, *SIARF4* overexpression plants; RNAi-8 and -18, *SIARF4* RNAi plants. The number of II type trichomes in an area of 0.5 cm² and the number of V and VI type trichomes in an area of 2.2 mm² were calculated under a light microscope. Each value indicates the mean \pm SE of three biological replicates. * and ** indicate significant difference between WT and transgenic leaves with $P < 0.05$ and $P < 0.01$, respectively, as determined by *t*-test.

leaves from the RNAi-*SIARF4* plants was higher than that of the spider mites that preferred the WT plants (Figures 2c and d). Spider mite inoculation assay was performed. The 10- and 25-day trials with adult female mites resulted in the localized collapse of the leaves of the RNAi-*SIARF4* lines and in small chlorotic lesions, which are indicative of mite feeding, in the leaves of the OE-*SIARF4* lines (Figure 2e). After 45 days of assays, severe damages were observed in the RNAi-*SIARF4* and WT plants and some plants died. By contrast, the inoculated leaves of OE-*SIARF4* lines remained green and had relatively few signs of macroscopic damage (Figure 2e). The ability of the spider mites to colonize the host was examined by measuring the fecundity of the female mites. The egg number laid on the OE-*SIARF4* plants was lower

than that on the WT plants, whereas the number of eggs laid on the RNAi-*SIARF4* plants was higher than that on the WT plants (Figure 2f). The overexpression of *SIARF4* in tomato increased spider mite tolerance, and the down-regulation of *SIARF4* increased the sensitivity of the tomato plants to spider mites.

***SIARF4* bound to the AuxRE and TGA motifs of the *SITHM1* and *SIMYB52* promoters, respectively, and inhibited their expression**

The differentially expressed genes (DEGs) between the WT and *SIARF4* RNAi lines were identified through RNA sequencing (RNA-Seq), using the leaves of 45-day-old tomato seedlings. A total of 398 DEGs, including 275 up-regulated and 123 down-regulated



genes, were identified (Table S1). Gene Ontology (GO) function and pathway enrichment analyses showed that the down-regulation of *SIARF4* influenced several metabolic pathways (Table S2, Figure S6 and S7a). Forty-nine DEGs belong to 16 TF families (Table S3). The dominant families included WRKY (nine DEGs), MYB (six DEGs), ERF (six DEGs), MIKC_MADS (five DEGs) and C2H2-type zinc-finger families (five DEGs; Figure S7b). *MYBs* play an important role in trichome formation (Machado *et al*, 2009; Wang *et al*, 2004). *SITHM1* (Solyc08g081500) and *SIMYB52* (Solyc03g093890) contained the AuxRE (TGCTC) motif

and auxin response element (TGA motif, AACGAC), respectively, which are the binding motifs of ARF proteins.

Both *SITHM1* and *SIMYB52* belong to R2R3MYB transcription factors family that plays regulatory roles in plant development and defence responses as one of the largest transcription factor families in tomato (Li *et al*, 2016; Zhao *et al*, 2014). *SITHM1* has an open reading frame (ORF) of 762 bp that encodes a protein containing 253 amino acid residues while *SIMYB52* has an open reading frame (ORF) of 996 bp that encodes a protein containing 331 amino acid residues. Phylogenetic analysis of tomato

Figure 2 Tolerance of SIARF4 plants to two-spotted spider mites and SIARF4 targets *SITHM1* and *SIMYB52*. a–d, Preference experiment to analyse the preference of spider mites for WT and SIARF4 plants. Ten adult female spider mites were positioned in an area that was equidistant from WT and SIARF4 leaflets. The number of mites that moved to different leaflets and those that failed to make a choice (nc) were counted 1 h after initiating the assay. The data represent the mean values \pm SE based on 16 experimental repetitions (total of 160 mites). e, Inoculation of WT and SIARF4 plants with two-spotted spider mites for 45 days. Fifteen adult female mites were transferred to a single leaf on 15-day-old WT and SIARF4 plants. f, Fecundity of two-spotted spider mites in the leaves of WT and SIARF4 plants. Five adult female mites moved to the leaf discs (12 mm) of WT and SIARF4 plants. Eggs were counted via a microscope at 24-h intervals for 4 days. WT, wild-type plants; OE-28 and -31, *SIARF4* overexpression plants; RNAi-8 and -18, *SIARF4*-down-regulated plants. The data represent the mean values and SE from 12 independent experiments. * and ** indicate significant difference between WT and *SIARF4* leaves with $P < 0.05$ and $P < 0.01$, respectively (*t* test). g and h, EMSA showing the direct binding of SIARF4 to the promoters of *SITHM1* and *SIMYB52*. Biotin-labelled DNA probes from original promoter or mutants were incubated with GST-SIARF4 protein, and then, DNA–protein complexes were separated on 6% native polyacrylamide gels. + or +++ indicates increasing amounts of unlabelled probes for competition. i and j, ChIP-qPCR assay for the direct binding of SIARF4 to the promoters of *SITHM1* and *SIMYB52*. Values represent the percentage of DNA fragments that co-immunoprecipitated with anti-SIARF4 antibodies or nonspecific antibodies (anti-IgG) comparative to the input DNA. The data are means \pm SE from qPCR of four biological replicates. k, Diagrams of the reporter and effector vectors in the dual-luciferase reporter assay. l, *SIARF4* suppresses the transcription of *SITHM1* and *SIMYB52*. The activities of firefly LUC and REN in tobacco leaves were measured and LUC/REN ratio was analysed after infiltration with *A. tumefaciens* carrying the reporter plasmid and different combinations of effector plasmids. Each value represents the mean of six biological replicates, and vertical bars represent the SE.

R2R3MYB family proteins revealed that *SITHM1* along with *SIMYB56*, *SIMYB67* and *SIMYB26* belong to S15 subgroup; *SIMYB52* along with *SIMYB51*, *SIMYB95* and *SIMYB105* belong to S6 subgroup (Zhao *et al.*, 2014). Amino acid sequence analyses of *SITHM1* and *SIMYB52* were conducted with known MYB proteins in the same subgroup, respectively (Figure S10). Both *SITHM1* and *SIMYB52* proteins contain an R2R3 domain in the N-terminus (Figure S10). In addition, phylogenetic trees of *SITHM1* and *SIMYB52* with homologous proteins from other species were also generated, respectively (Figure S11). *SITHM1* is closely related to *SbMYB21* while *SIMYB52* is closely related to *SpMYB15*, indicating possible functional similarity among them.

The direct binding of SIARF4 protein to *SITHM1* and *SIMYB52* genes was verified by electrophoretic mobility shift assay (EMSA). Purified recombinant truncated SIARF4 and glutathione S-transferase (GST) fusion protein (GST-tSIARF4) were successfully obtained (Figure S8). The GST-tSIARF4 fusion protein bound to biotin-labelled probes containing AuxRE and TGA motifs that were derived from *SITHM1* and *SIMYB52* promoters, respectively, and caused a mobility shift that was effectively abolished in a dose-dependent manner when unlabelled *SITHM1* and *SIMYB52* promoter fragments were added as competitors (Figures 2g and h). Mobility shift was not observed when biotin-labelled probes were incubated with GST only (Figures 2g and h). This finding indicated that the specific targets of SIARF4 were *SITHM1* and *SIMYB52*. Chromatin immunoprecipitation coupled with quantitative polymerase chain reaction (ChIP-qPCR) was used in confirming the interaction between SIARF4 and the *SITHM1* and *SIMYB52* genes *in vivo*. The promoter regions of *SITHM1* and *SIMYB52* were specifically enriched when FLAG antibodies were used instead of nonspecific antibodies (IgG; Figures 2i and j). SIARF4 possessed transcriptional repression activity and directly targeted the promoters of *SITHM1* and *SIMYB52*. Hence, the transcriptional repression of *SITHM1* and *SIMYB52* by SIARF4 were determined through transient dual-luciferase assays. The overexpression of *SIARF4* remarkably reduced luciferase activity driven by the promoters of *SITHM1* and *SIMYB52* compared with the vector control (pEAQ; Figures 2k and l). qRT-PCR showed that the expression levels of *SITHM1* and *SIMYB52* increased in the RNAi-SIARF4 plants but decreased in the OE-SIARF4 plants (Figure S9). The results indicated that SIARF4 targeted *SITHM1* and *SIMYB52* repressed their transcription.

SITHM1 negatively affected the auxin-induced formation of II and VI type trichomes in the leaves

qRT-PCR was performed to assess the expression pattern of *SITHM1* (Figure S12). *SITHM1* was expressed in all tissue tested with the highest expression in leaf trichomes. GUS staining showed that *SITHM1* was specifically expressed in II and VI type trichomes but not in V type trichome (Figure 3a). *SITHM1*-green fluorescent protein (GFP) was transiently expressed in the leaf epidermal cells of tobacco for subcellular localization, and fluorescence signals were detected in the nucleus, indicating that the *SITHM1* was localized in the nucleus of plant cells (Figure 3b). The transcriptional activity of *SITHM1* in tobacco leaves was analysed using a dual-luciferase reporter system. *SITHM1* increased the LUC/REN ratio compared with the empty vector pBD, revealing that *SITHM1* possesses transcriptional activation activity (Figure S13).

The *SITHM1* function on trichome formation was analysed in using RNAi strategy. The homozygous transgenic lines of RNAi-SITHM1 showed a substantially low degree of *SITHM1* transcript accumulation (Figure 3c). Without IAA treatment, RNAi-SITHM1 plants exhibited increases in the densities of II and VI type trichomes in leaves and no change in V type trichome compared with WT plants (Figures 3d and e). The density of epidermal pavement cells was analysed, and results showed that the down-regulation of *SITHM1* increased the density of the epidermal pavement cells of the tomato leaves (Figure S14). An apparent increase in the number of II and VI type trichomes per epidermal cell in RNAi-SITHM1 lines was observed (Figure 3f). These results indicated that *SITHM1* negatively affected the formation of II and VI type trichomes. RNAi-SITHM1 plants with IAA treatment showed obvious increases in the densities of II, V and VI type trichomes in the tomato leaves (Figure 3g). The trichome density ratio between IAA treatment to no-IAA treatment was calculated, showing that the density ratios of II and VI type trichomes on the RNAi-SITHM1 plants were higher than those of the WT plants and that the density ratio of V type trichome was similar to that of the WT plants (Figure 3h). The down-regulation of *SITHM1* increased the effect of IAA treatment on the formation of II and VI type trichomes. Our results demonstrated that *SITHM1* regulated the auxin-induced formation of II and VI type trichomes in tomato leaves.

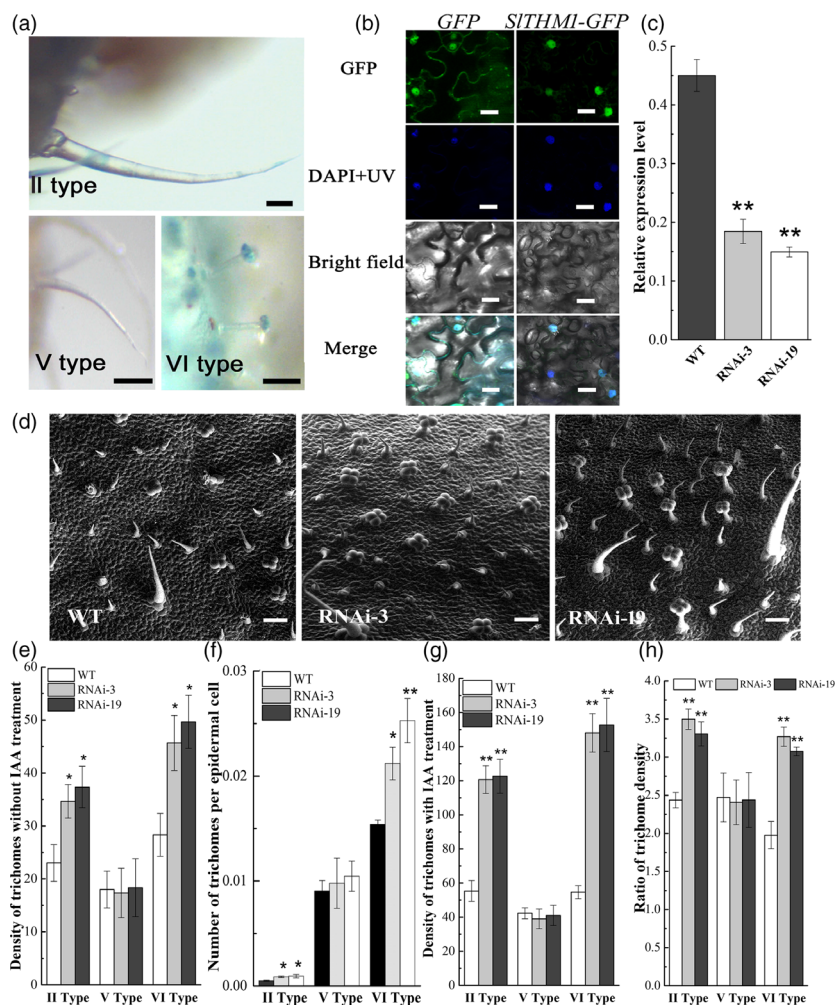


Figure 3 Expression analysis of *SITHM1*, subcellular localization analysis of *SITHM1* protein, transcriptional activation and trichome density of the leaves of RNAi-*SITHM1* plants. a, Expression pattern of *SITHM1* in trichome tissues explored by GUS reporter gene expression driven by the *SITHM1* promoter. Scale bars = 0.2 mm. b, Subcellular localization analysis of *SITHM1*. Tobacco leaves were transiently transformed with empty GFP vector and *SITHM1*-GFP construct via *A. tumefaciens* transfection. A fluorescence microscope was used to observe GFP fluorescence. *35S::GFP* was used as positive control. Scale bars = 15 μ m. c, qRT-PCR analysis of the expression of *SITHM1* gene in RNAi-*SITHM1* plants. The data are the means \pm SE from qPCR of four biological replicates. d, Scanning electron micrographs of the leaf surface. Scale bars = 60 μ m. e, Density analysis of II, V and VI type trichomes from the leaves of WT and *SITHM1* RNAi plants without IAA treatment. Scale bars = 0.2 mm. f, Number of trichomes per epidermal cell of the leaves of WT and RNAi-*SITHM1* tomato plants without IAA treatment. g, Density analysis of II, V and VI type trichomes in the leaves of WT and *SITHM1* lines with IAA treatment. h, Trichome density ratio of IAA treatment to no-IAA treatment. WT, wild-type plants; RNAi-3 and RNAi-19, *SITHM1*-down-regulated plants. The number of II type trichomes in an area of 0.5 cm² and the number of V and VI types trichomes in an area of 2.2 mm² were calculated under a light microscope. All experiments were replicated three times. * and ** indicate significant difference between WT and transgenic leaves with $P < 0.05$ and $P < 0.01$, respectively, as determined by *t*-test.

Down-regulation of *SITHM1* conferred spider mite tolerance to tomato

Spider mites were used in analysing the response of the RNAi-*SITHM1* lines to herbivores. Spider mite preference experiment showed that the number of spider mites that preferred RNAi-*SITHM1* leaves was lower than that of the mites that preferred the leaves of the WT plants (Figures 4a and b). Spider mite inoculation assay was carried out. The localized collapse of the WT leaves was obvious, but only small chlorotic lesions indicative of mite feeding was apparent on the RNAi-*SITHM1* leaf tissues after 25 days (Figure 4c). After 45 days, spider mites caused severe damage and nearly killed the WT plants, but the RNAi-*SITHM1* plants survived and retained some green leaves

(Figure 4c). Furthermore, the number of eggs laid on the RNAi-*SITHM1* leaves was remarkably lower than that on the WT leaves during the 4-day assay (Figure 4d). The results indicated that the down-regulation of *SITHM1* in tomato improved tolerance to spider mites.

SIMYB52 negatively regulated the auxin-induced formation of V type trichome in tomato leaves

qRT-PCR and GUS staining were used to explore the expression pattern of *SIMYB52* (Figures 5a, S15). GUS staining showed that *SIMYB52* was specifically expressed in the V type trichome of leaves (Figure 5a). Subcellular localization assay of *SIMYB52* showed that *SIMYB52* was localized in the nucleus of plant cells (Figure 5b). RNAi-*SIMYB52* transgenic lines were generated to

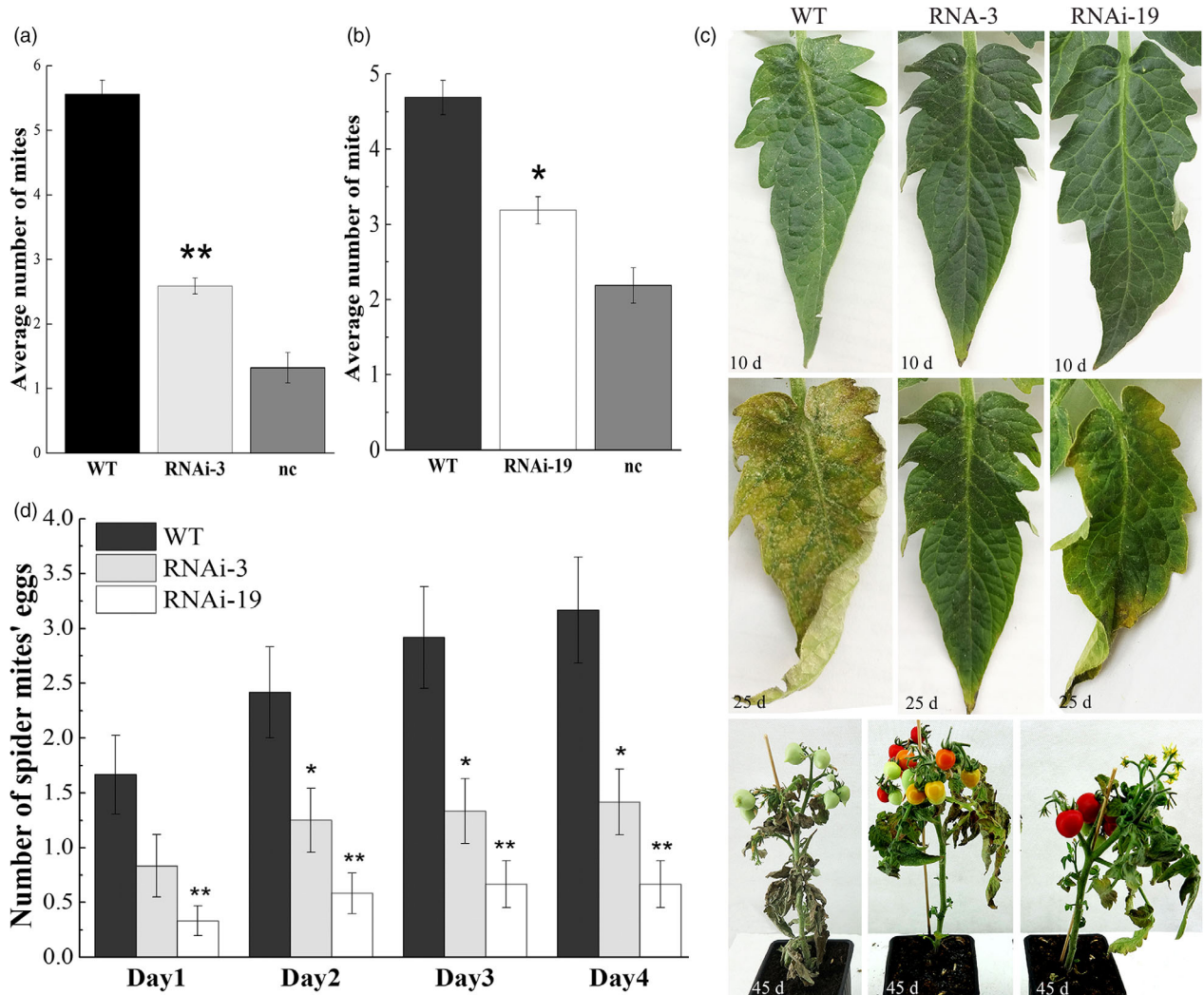


Figure 4 Tolerance of *SITHM1* RNAi plants to two-spotted spider mites. a and b, Spider mite preference experiment to measure the preference of spider mites for WT and *SITHM1* plants. The data represent the mean values and SE based on 16 experimental repetitions (total of 160 mites). c, Inoculation of WT and *SITHM1* RNAi plants with two-spotted spider mites for 45 days. Photographs of the infested leaves and whole plants were obtained after treatment. d, Fecundity of two-spotted spider mites on WT and *SITHM1* plants. The data are the mean values and SE from 12 independent experiments. WT, wild-type plants; RNAi-3 and RNAi-19, RNAi-*SITHM1* plants.

analyse the functions of *SIMYB52* on trichome formation in tomato. The homozygous transgenic lines of RNAi-*SIMYB52* showed a substantially low degree of *SIMYB52* transcript accumulation and obvious increase in the density of V type trichome (Figures 5c–e). The down-regulation of *SIMYB52* increased the density of epidermal pavement cells of tomato leaves (Figure S16). Then, the calculated number of trichomes per epidermal cell of RNAi-*SIMYB52* lines indicated an apparent increase in the number of V type trichomes per epidermal cell in the leaves (Figure 5f). Our data indicated that *SIMYB52* negatively affected the formation of V type trichome in the tomato leaves. RNAi-*SIMYB52* plants with IAA treatment showed obvious increases in the densities of II, V and VI type trichomes in the leaves (Figure 5g). The calculated trichome density ratio between the IAA treatment and no-IAA treatment of V type trichomes in the RNAi-*SIMYB52* plants were higher than that in the WT plants, and the ratios of II and VI type trichomes in the RNAi-*SIMYB52* plants were similar with the ratio in the WT plants (Figure 5h). The down-regulation of *SIMYB52* increased the effect of IAA

treatment on the formation of V type trichomes in the tomato leaves, and *SIMYB52* was involved in the auxin-induced formation of V type trichome in tomato leaves.

Spider mite inoculation assay, preference assay and fecundity assay were conducted to analyse the response of RNAi-*SIMYB52* plants to spider mites. RNAi-*SIMYB52* plants showed no change in the response to spider mite compared with WT plants (Figure S17a, b, c).

SIARF4 depended on *SITHM1* to regulate type II and VI trichome formation

The OE-*SIARF4* and RNAi-*SIARF4* lines were separately crossed with the RNAi-*SITHM1* line to further explore the interaction between *SIARF4* and *SITHM1* in the formation of type II, V and, VI trichomes. The densities of II and VI type trichomes in RNAi-*SITHM1* and OE-*SIARF4* crossed (OE-*SIARF4*♂RNAi-*SITHM1*♀) lines without IAA treatment were similar to those in RNAi-*SITHM1* and OE-*SIARF4* lines and higher than those in the WT plants (Figure 6a). The densities of V type trichomes on OE-

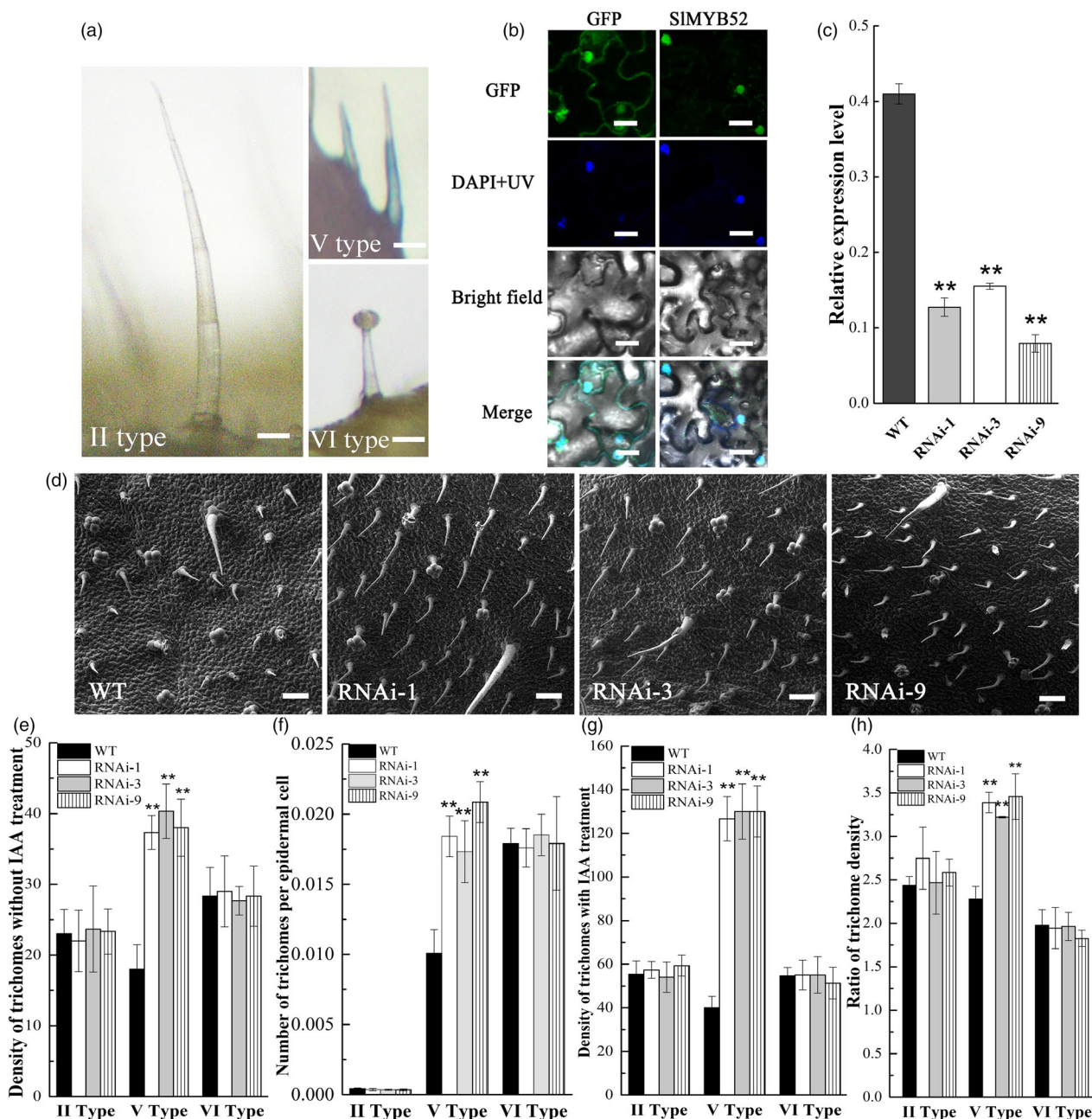


Figure 5 Expression analysis of *SIMYB52*, subcellular localization analysis of *SIMYB52* protein and trichome density of leaves in *SIMYB52* plants. a, Expression pattern of *SIMYB52* in trichome tissues explored by GUS reporter gene driven by the *SIMYB52* promoter. Scale bars = 0.2 mm. b, Subcellular localization analysis of *SIMYB52* in tobacco leaves. 35S: GFP was used as positive control. Scale bars = 15 μ m. c, qRT-PCR analysis of the expression of *SIMYB52* in RNAi plants. d, Scanning electron micrographs of the leaf surface. Scale bars = 60 μ m. e, Density analysis of II, V and VI type trichomes from the leaves of WT and *SIMYB52* RNAi plants without IAA treatment. Scale bars = 0.2 mm. f, Number of trichomes per epidermal cell of tomato leaves from WT and RNAi-*SIMYB52* plants without IAA treatment. g, Density analysis of II, V and VI type trichomes in the leaves of WT and *SIMYB52* lines with IAA treatment. h, Trichome density ratio of IAA treatment to no-IAA treatment. Number of II type trichomes in an area of 0.5 cm² and number of V and VI type trichomes in an area of 2.2 mm² were calculated under a light microscope. WT, wild-type plants; RNAi-1, RNAi-3 and RNAi-9, RNAi-*SIMYB52* plants. All experiments were replicated three times. ** represent significant difference between WT and transgenic leaves with $P < 0.01$ (t -test).

SIARF4 σ RNAi-SITHM1 η lines increased compared with those on RNAi-SITHM1 and WT lines and were similar with those in the OE-SIARF4 lines. Moreover, the densities of II and VI type trichomes in RNAi-SITHM1 and RNAi-SIARF4 crossed (RNAi-SIARF4 σ RNAi-SITHM1 η) lines were increased compared with those in the RNAi-SIARF4 and WT lines and were similar to those in the RNAi-

SITHM1 and OE-SIARF4 lines. The densities of V type trichome in the RNAi-SIARF4 σ RNAi-SITHM1 η lines were lower than those in the RNAi-SITHM1 and WT lines and similar to those in the RNAi-SIARF4 lines (Figure 6a). Hybrid experiments showed that the down-regulation of *SITHM1* specifically increased II and VI type trichomes in the *SIARF4* down-regulation background. *SIARF4*

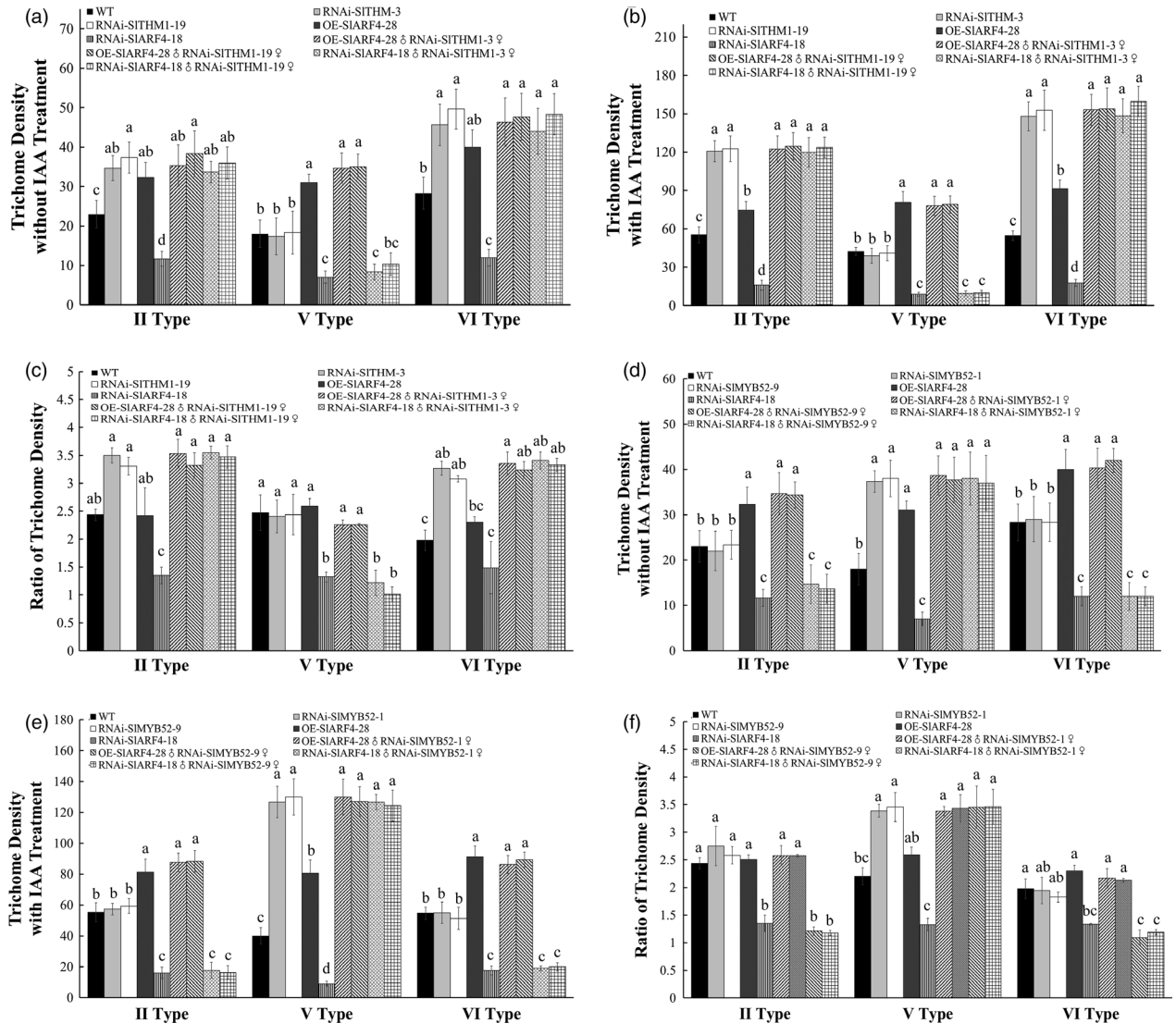


Figure 6 Density analysis of II, V and VI type trichomes from the leaves of crossed plants among OE-SIARF4, RNAi-SIARF4, RNAi-SITMH1 and RNAi-SIMYB52 plants. a, Trichome densities of crossed plants between OE-SIARF4 or RNAi-SIARF4 and RNAi-SITMH1 plants without IAA treatment. b, Trichome densities of crossed plants between OE-SIARF4 or RNAi-SIARF4 and RNAi-SITMH1 plants with IAA treatment. c, Trichome density ratio of IAA treatment to no-IAA treatment. d, Trichome densities of crossed plants between OE-SIARF4 or RNAi-SIARF4 and RNAi-SIMYB52 plants without IAA treatment. e, Trichome densities of crossed plants between OE-SIARF4 or RNAi-SIARF4 and RNAi-SIMYB52 plants with IAA treatment. f, Trichome density ratio of IAA treatment to no-IAA treatment. Number of II type trichomes in an area of 0.5 cm² and number of V and VI type trichomes in an area of 2.2 mm² were calculated under a light microscope. All experiments were replicated three times. Significant differences (Tukey's multiple range test, $P < 0.05$) are indicated in lowercase.

induced the formation of II and VI type trichomes and was dependent on *SITMH1*.

The densities of II, V and VI type trichomes in the OE-SIARF4 σ RNAi-SITMH1 ρ and RNAi-SIARF4 σ RNAi-SITMH1 ρ lines with IAA treatment increased compared with the plants without IAA treatment (Figure 6b). The trichome density ratios between IAA treatment and no-IAA treatment were calculated. The density ratios of II and VI type trichomes on OE-SIARF4 σ RNAi-SITMH1 ρ and RNAi-SIARF4 σ RNAi-SITMH1 ρ lines were similar to those in the RNAi-SITMH1 plants and higher than those in the OE-SIARF4, RNAi-SIARF4 and WT plants (Figure 6c). The density ratios of V type trichome in OE-SIARF4 σ RNAi-SITMH1 ρ were similar to those in the OE-SIARF4 plants, and the density ratios of V type trichomes in the RNAi-SIARF4 σ RNAi-SITMH1 ρ lines were similar to those in the RNAi-SIARF4 plants (Figure 6c). The down-

regulation of *SITMH1* gene specifically increased the IAA-induced formation of II and VI type trichomes in the SIARF4 down-regulation background, and the regulation of SIARF4 in the auxin-induced formation of II and VI type trichomes was dependent on *SITMH1* in tomato.

SIARF4 depended on SIMYB52 to regulate V type trichome formation

OE-SIARF4 and RNAi-SIARF4 lines were separately crossed with RNAi-SIMYB52 lines. The densities of V type trichomes on RNAi-SIMYB52 and OE-SIARF4 crossed (OE-SIARF4 σ RNAi-SIMYB52 ρ) lines without IAA treatment were similar to those in the RNAi-SIMYB52 lines and higher than those in the WT plants (Figure 6d). The densities of II and VI type trichomes in the OE-SIARF4 σ RNAi-SIMYB52 ρ lines increased compared with those in

the RNAi-SIMYB52 and WT lines and were similar to those in the OE-SIARF4 lines (Figure 6d). Moreover, the densities of V type trichomes in RNAi-SIMYB52 and RNAi-SIARF4 crossed (RNAi-SIARF4 σ RNAi-SIMYB52 φ) lines increased compared with those in the RNAi-SIARF4 and WT lines and were similar to those in the RNAi-SIMYB52 and OE-SIARF4 plants (Figure 6d). The densities of II and VI type trichomes in the RNAi-SIARF4 σ RNAi-SIMYB52 φ lines were lower than those in the RNAi-SIMYB52, OE-SIARF4 and WT lines and similar to those in the RNAi-SIARF4 plants (Figure 6d). Cross experiments showed that the down-regulation of *SIMYB52* gene specifically increased the formation of V type trichome in the SIARF4 down-regulation background. The regulation of SIARF4 in the formation of V type trichomes in tomato was dependent on SIMYB52.

The densities of II, V and VI type trichomes in the OE-SIARF4 σ RNAi-SIMYB52 φ and RNAi-SIARF4 σ RNAi-SIMYB52 φ lines with IAA treatment obviously increased compared with those in plants without IAA treatment (Figure 6e). The trichome density ratios between the IAA treatment and no-IAA treatment were calculated. The density ratios of V type trichomes in the OE-SIARF4 σ RNAi-SIMYB52 φ and RNAi-SIARF4 σ RNAi-SIMYB52 φ lines were similar to those in the RNAi-SIMYB52 plants and higher than those in the OE-SIARF4, RNAi-SIARF4 and WT plants (Figure 6f). The density ratios of II and VI type trichomes in the OE-SIARF4 σ RNAi-SIMYB52 φ plants were similar to those in the OE-SIARF4 plants, and the ratios of II and VI type trichomes in the RNAi-SIARF4 σ RNAi-SIMYB52 φ lines were similar to those in the RNAi-SIARF4 plants (Figure 6f). The down-regulation of *SIMYB52* gene specifically increased the IAA-induced formation of V type trichome in the SIARF4 down-regulation background, and the regulation of SIARF4 in the auxin-induced formation of V type trichomes was dependent on SIMYB52 in tomato.

SITHM1 and SIMYB52 positively regulated the expression of *SICyCB2*

SICyCB2, a B-type cyclin gene, plays key roles in trichome initiation (Gao *et al.*, 2017). The promoter of *SICyCB2* contains an MYB-binding motif (AC-rich). The expression levels of *SICyCB2* decreased in the SITHM1 and SIMYB52 RNAi plants (Figure S18). The direct bindings of SITHM1 and SIMYB52 to *SICyCB2* promoter were analysed by EMSA. Purified recombinant truncated SITHM1, SIMYB52 and GST fusion proteins (GST-tSITHM1 and GST-tSIMYB52) were obtained (Figure S19). GST-tSITHM1 and GST-SIMYB52 fusion proteins bound to biotin-labelled probes containing the AC-rich motifs of the promoters of *SICyCB2* (Figures 7a and b), indicating the specific targets of SITHM1 and SIMYB52 to the promoters of *SICyCB2*. Transient dual-luciferase assay was used in determining the transcriptional regulation of *SICyCB2* by SITHM1 and SIMYB52. The overexpression of SITHM1 and SIMYB52 remarkably increased luciferase activity driven by *SICyCB2* promoters compared with the empty control vector (pEAQ) (Figures 7c and d), and SITHM1 and SIMYB52 increased the transcription of *SICyCB2*.

Discussion

Increased trichome density confers spider mite tolerance

The two-spotted spider mite is a ruthless pest that damages more than 140 plant families and 1100 plant species, including tomato (Dermauw, *et al.*, 2013). Spraying synthetic acaricides is primary performed to inhibit spider mite infestation. The drawback to the use of synthetic acaricides is that spider mites have the ability to

upsurge resistance to acaricides (Dermauw, *et al.*, 2013; Van Leeuwen *et al.*, 2004). An imperative substitute approach to beating spider mites is the breeding of tomato cultivars with resistance to spider mites (Johnson, 1992).

Elevated trichome density hampers pest feeding and migration and diminishes herbivore populations (Handley *et al.*, 2005; Horgan *et al.*, 2009). VOCs by glandular trichomes fend off or destroy pests (Schilmiller *et al.*, 2010). In this study, the overexpression of *SIARF4* amplified the densities of II, V and VI type trichomes and the tolerance of tomato to spider mites (Figures 1 and 2). Furthermore, the down-regulation of *SITHM1*, a repressor of trichome formation, increased the densities of II and VI type trichomes and tolerance to spider mites (Figures 3 and 4). However, the RNAi-SIMYB52 plants with increased density of V type trichome did not exhibit increase in tolerance to spider mite compared with the WT plants (Figure S17). Our study confirmed the positive correlation between trichome density and spider mite tolerance and demonstrated that the regulation of trichome densities by genetic engineering is an effective strategy for increasing plant resistance to herbivores. In addition, the major agricultural traits of the transgenic plants were also analysed. No significant difference was detected between transgenic and WT plants (Figures S20, S21 and S22), indicating that the R2R3 MYB-dependent auxin signalling may not be involved in the regulation of some other agricultural traits.

Auxin triggers the formation of unicellular and multicellular trichomes via *SIARF4*

Hormones regulate trichome formation, and different hormones stimulate different type of trichomes in tomato (Maes and Goossens, 2010). The utilization of JA application promotes the creation of multicellular I and VI type trichomes and unicellular V type trichome (Maes *et al.*, 2010), whereas cytokinin and gibberellin cause the creation of I type trichomes in tomato (Maes *et al.*, 2010). Given the fact that both auxin and JA play key roles in trichome formation, the expression levels of *SIARF3*, *SIARF4*, *SITHM1*, *SIMYB52* and *SICyCB2* in response to auxin and JA treatments were analysed by qRT-PCR (Figures S23, S24). All five genes showed response to IAA treatment, with *SIARF4* showing the highest up-regulation whereas *SIARF3* displayed slight up-regulation (Figure S23). On the other hand, *SITHM1*, *SIMYB52* and *SICyCB2* were down-regulated in response to IAA treatment (Figure S23). Moreover, *SIARF3*, *SIARF4*, *SITHM1* and *SIMYB52* were barely responsive to JA treatment while *SICyCB2* manifested mild down-regulation (Figure S24). In this study, auxin promoted the formation of unicellular V type trichome and multicellular II and VI type trichomes. *SIARF4* positively modulates the formation of II, V and VI type trichomes, and the down-regulation of *SIARF4* decreases the effect of IAA treatment on the formation of II, V and VI type trichomes (Figure 1). Our results demonstrated that auxin induced the formation of II, V and VI type trichomes in tomato leaves by promoting *SIARF4* expression. In addition, IAA treatment also increased the density of trichomes in RNAi-SIARF4 and *Slarf4* plants, which suggested that, other than *SIARF4*, there might be another regulatory pathway in controlling trichome formation. Further research will be needed to examine trichome formation in response to IAA treatment.

It is noteworthy that another auxin-responsive gene, *SIARF3*, is involved in the formation of epidermal cells and trichomes (Zhang *et al.*, 2015). The relation between *SIARF3* and *SIARF4* in regulating trichome formation was explored by multiple

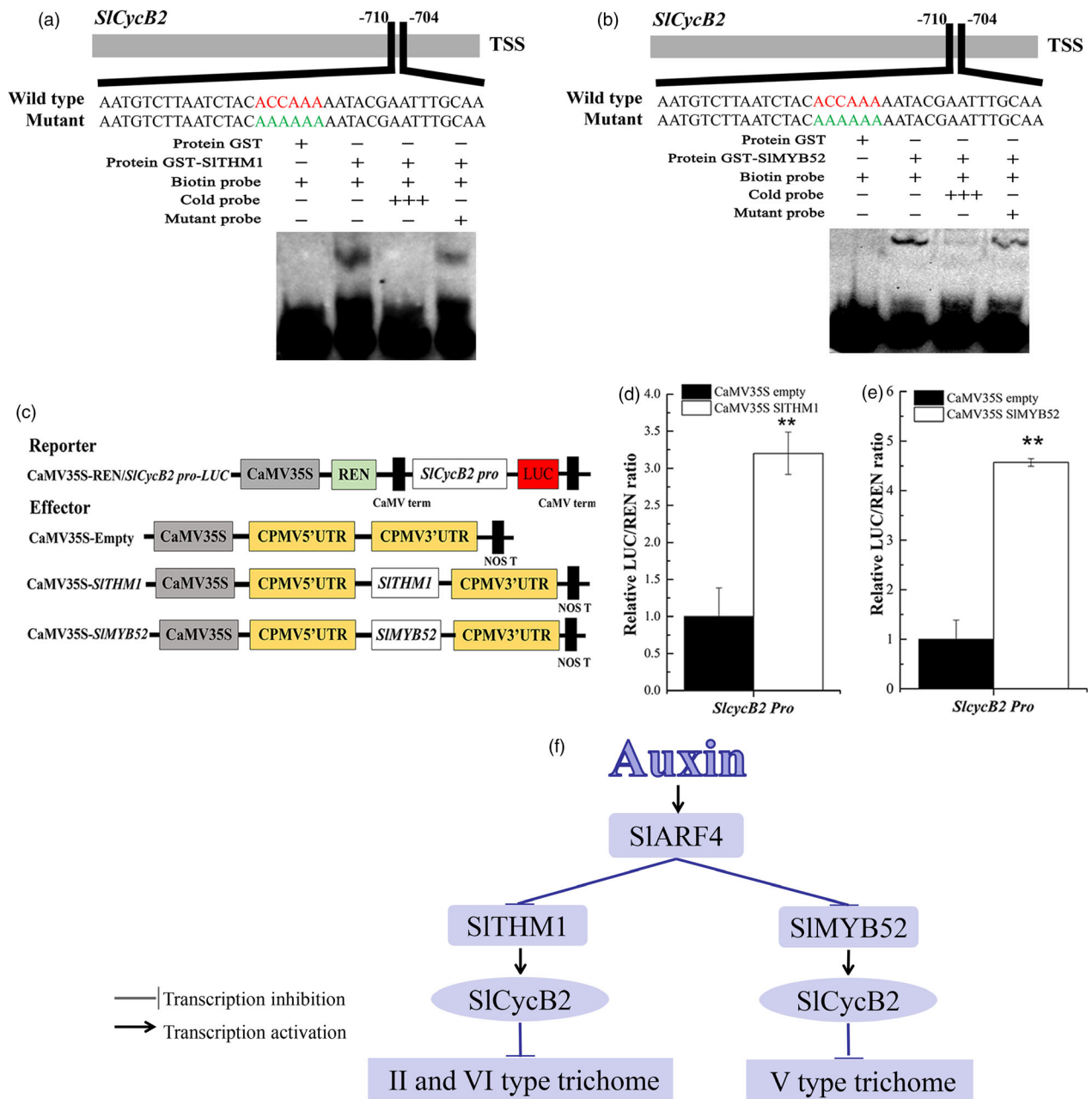


Figure 7 SITHM1 and SIMYB52 target *SlCycB2* and working model for R2R3 MYB-dependent auxin signalling pathway. a and b, EMSA showing the direct binding of SITHM1 and SIMYB52 to *SlCycB2* promoters. + or +++ indicates increasing amounts of unlabelled probes for competition. c, Diagrams of reporter and effector vectors in the dual-luciferase reporter assay. d, SITHM1 increases the transcription of *SlCycB2*. e, SIMYB52 increases the transcription of *SlCycB2*. Each value represents the mean of six biological replicates, and vertical bars represent the SE. f, Working model. Auxin induces the expression of *SlARF4* gene, and *SlARF4* protein inhibits the expressions of *SITHM1* and *SIMYB52* genes. The inhibited *SITHM1* levels reduce the *SlCycB2* expression, which promotes the formation of II and VI type trichomes. The inhibited *SIMYB52* levels reduce the *SlCycB2* expression, which promotes the formation of V type trichome.

approaches. The expression level of *SlARF3* was first assessed in *SlARF4* transgenic lines (Figure S25). qRT-PCR results revealed that there was no significant change of the expression level of *SlARF3* in *SlARF4* transgenic lines, suggesting that *SlARF3* and *SlARF4* could function independently in regulating trichome formation. Next, further examination of both proteins reveals that, *SlARF4* protein has typical domains (B3, ARF and Aux/IAA) while *SlARF3* only contains two conserved domains, B3 and ARF

(Zhang et al., 2015). Furthermore, we generated *SlARF3/4* double knockdown tomato plants by crossing RNAi-*SlARF3* and RNAi-*SlARF4* transgenic lines. These plants exhibited significant lower trichome density, epidermal cell density and number of trichomes per epidermal cells compared with the parent lines (Figures S26, S27 and S28). Finally, RNA-Seq analyses of RNAi-*SlARF3* and RNAi-*SlARF4* plants revealed that *SlARF3* and *SlARF4* regulate the different set of down-stream genes (data not shown). These

results demonstrate that *SIARF3* and *SIARF4* play different regulatory roles in regulating trichome formation.

SIARF4 regulates the auxin-induced formation of unicellular and multicellular trichomes through the transcriptional inhibition of *SIMYB52* and *SITHM1*

Numerous overexpressed genes linked to unicellular trichomes in *Arabidopsis* negate the same result for Solanaceae species with multicellular trichome formation (Payne *et al.*, 1999). In *Arabidopsis*, the overexpression of *MIXTA* and *AmMYBML1*, which are multicellular trichome-related genes, did not prompt the formation of unicellular trichomes (Glover *et al.*, 1998), whereas the interaction between *Wo* and *SlCycB2* regulated trichome formation in tomato (Yang *et al.*, 2011). The promotion of trichome formation was not observed in *Arabidopsis* with overexpressed *Wo* gene (Yang and Ye, 2013). These reported data implied tomato and tobacco multicellular trichomes and *Arabidopsis* unicellular trichomes employ different regulatory pathways (Yang and Ye, 2013).

SIARF4 regulated the formation of unicellular and multicellular trichomes. *SIARF4* negatively regulated *SITHM1* and *SIMYB52* expression by binding to AuxRE and TGA motifs, respectively (Figure 2). *SITHM1* functioned as a repressor in the regulation of the formation of II and VI type trichomes, and *SIMYB52* acted as a repressor during V type unicellular trichome formation. qRT-PCR showed that the expression levels of *SITHM1* and *SIMYB52* increased in the RNAi-*SIARF4* plants and decreased in the OE-*SIARF4* plants (Figure S9). Hybrid experiments showed down-regulation of *SITHM1* specifically increased the formation of II and VI type trichomes, and *SIMYB52* specifically increased the formation of V type trichome in the *SIARF4* down-regulation background (Figure 6). *SIARF4* modulated the formation of II, V and VI type trichomes depending on *SITHM1* and *SIMYB52*. II and V type trichomes are nonglandular, whereas V type is glandular (Deng *et al.*, 2012). *SIARF4* positively regulated the formation of unicellular and multicellular trichomes through the direct transcriptional inhibition of *SIMYB52* and *SITHM1*. Our study demonstrated the presence of consistent but different characteristics in the regulation of unicellular and multicellular trichome formation in tomato leaves.

Compared with *SlUBI* expression, real expression levels of *SITHM1* and *SIMYB52* are not very high in the tomato leaf tissue (Figures 3c,5c). Furthermore, *SITHM1* had highest expression level in leave trichomes (Figure S12) and *SIMYB52* had relatively high expression level in leaves (Figure S15). These facts indicate that there might be other regulatory mechanisms in regulation trichome formation. Protein translation regulation and post-translation regulation also impact the actual protein levels of *SITHM1* and *SIMYB52* in regulating trichome formation. In addition, besides R2R3 MYB-dependent auxin signalling, there should exist other regulatory pathways in regulating trichome formation, such as JA signalling pathway.

The down-regulation of *SITHM1* increased the effect of IAA treatment on the formation of II and VI type trichomes, and the down-regulation of *SIMYB52* increased the effect of IAA treatment on the formation of V type trichome (Figures 3 and 5). *SITHM1* and *SIMYB52* were involved in the auxin-induced formation of II, V and VI type trichomes in tomato leaves. Our results demonstrated the important roles of *SIARF4*, *SITHM1* and *SIMYB52* in the auxin-mediated transcriptional regulation of unicellular and multicellular trichome formations in tomato leaves.

SITHM1* and *SIMYB52* regulate trichome formation by directly binding to *SlCycB2

Cyclins are involved in the transition between the phases of the cell cycle in eukaryotes and function as the positive regulators of cell proliferation (Meijer and Murray, 2001). B-type cyclins play important roles in G2/M transition (Fobert *et al.*, 1994; Hirt *et al.*, 1992). In *Arabidopsis*, the specific expression of B-type cyclin B1:2 induces the formation of multicellular trichomes; hence, B-type cyclins play important roles in unicellular and multicellular trichome formation (Schnittger *et al.*, 2002). In tomato, *Wo* protein interacts with *SlCycB2*, which is essential for type I trichome formation (Yang *et al.*, 2011). The overexpression of *SlCycB2* decreases the levels of glandular I and VI type trichomes and all nonglandular trichomes. On the other hand, the suppression of *SlCycB2* promotes the formation of nonglandular III and V type trichomes on Ailsa Craig tomato (Gao *et al.*, 2017). Hence, *SlCycB2* may function as an inhibitor in the formation of glandular and nonglandular trichomes (Gao *et al.*, 2017). In the present study, *SITHM1* and *SIMYB52* functioned as repressors in the formation of multicellular and unicellular trichomes (Figures 3 and 5). *SITHM1* and *SIMYB52* directly targeted the *SlCycB2* and activated its expression (Figure 7). We anticipated that *SITHM1* and *SIMYB52* regulate trichome formation through the activation of *SlCycB2* that may act as a repressor in the formation of unicellular and multicellular trichomes in 'Micro-Tom' tomato cultivar. Future study could focus on functional analysis of *SlCycB2* in 'Micro-Tom' using CRISPR/Cas9 technology.

We proposed a model of how auxin induces the formation of II, V and VI type trichomes in tomato leaves. Auxin induces the expression of *SIARF4*, and *SIARF4* protein inhibits the expressions of *SITHM1* and *SIMYB52*. Decreased *SITHM1* levels reduce *SlCycB2* expression, which promotes the formation of II and VI type trichomes. Decreased *SIMYB52* levels inhibit *SlCycB2* expression, resulting in the promotion of the formation of V type trichomes (Figure 7). The *SITHM1/SIMYB52*-dependent auxin signalling pathway modulates the formation of unicellular and multicellular trichomes in tomato, and increasing trichome density is an effective method to improve the tolerance of tomato to spider mites.

Methods

Plant material and growth conditions

Tomato (*Solanum lycopersicum* 'Micro-Tom') plants were used. 'Micro-Tom' is a typical laboratorial tomato cultivar because of its short life cycle and efficient genetic transformation system. Standard greenhouse conditions are 14-h day/10-h night cycle, 25°C/20°C day/night temperature, 80% relative humidity (RH) and 250 mol/m²/s intense luminosity. Major agricultural traits were measured as previously described by Lovelli *et al.*, 2012.

Sequence analysis

Sequence analysis was performed according to Zhang *et al.* (2015). GenBank accession numbers for the alignment as well as phylogenetic analysis are presented in supplementary materials.

Trichome counts and phenotyping

Forty-five-day-old tomato seedlings were used for trichome counts. Fully expanded leaves were collected from the fifth internode counted from the shoot tip. Samples were dissected from midway between the margin and midrib in 10 mm × 4 mm

strips covering the whole leaf blade (avoiding the primary veins). II, V and VI type trichomes on the adaxial leaf surfaces were analysed under a JNOEC JSZ5B stereo microscope and a HITACHI TM400 plus scanning electron microscope. The numbers of type II trichomes in an area of 0.5 cm² and the numbers of V and VI type trichomes in an area of 2.2 mm² were calculated. Adaxial epidermal pavement cells were analysed through colourless nail polish printing mark method.

Auxin and JA treatment

Indole acetic acid (IAA) and jasmonate acid (JA) were purchased from Sigma company. Fifteen-day-old tomato seedlings for auxin treatment were sprayed with IAA solution (0, 1, 10, 30, 50 mg/L) every 2 days for 1 month. Four tomato seedlings were used for each group, and three groups were used for each treatment. Trichome analysis was conducted 1 month after the first spray. IAA solution (30 mg/L) was used in subsequent experiments in this study. For qRT-PCR analysis, JA solution (100 µM) and IAA solution (30 mg/L) were used. Chemical induction of 3-week-old tomato plants was conducted by dipping the tomato leaf in a solution containing either IAA or JA. Leaves from four WT were collected at three time points (0 h, 2 h and 6 h) during IAA and JA treatments, and frozen immediately in liquid nitrogen for RNA extraction.

Subcellular localization of SITHM1 and SIMYB52

Subcellular localization assays were conducted in tobacco (*Nicotiana benthamiana*) leaves. The coding regions of SITHM1 and SIMYB52 without a stop codon were cloned into the pCX-DG vector in frame with the GFP sequence and cauliflower mosaic virus (CaMV) 35S promoter. *Agrobacterium tumefaciens* strain GV3101, which carried the fusion constructs and the control GFP vector (pCX-DG frame), were infiltrated into the abaxial air space of 4- to 6-week-old tobacco plants, using a needleless 2-mL syringe. GFP fluorescence was observed using a laser scanning confocal microscope. All transient expression assays were repeated at least three times. The primers used are listed in Table S4.

Generation of transgenic plants

The open reading frame sequence of *SIARF4* was amplified and cloned into plant binary vector pLP100 to obtain *SIARF4* overexpression vector. RNAi vector was constructed by cloning the target sequences of *SIARF4*, *SITHM1* and *SIMYB52* into pCAMIBA2301. GUS staining vector was constructed by cloning the 2 kb promoter sequences of *SITHM1* and *SIMYB52* into the pLP100 vector that contain *GUS* reporter gene. Transgenic plants were obtained via *A. tumefaciens*-mediated method based on Zhang *et al.*, 2015. All experiments were conducted using homozygous lines from T3 generations. The primers used are listed in Table S4.

qRT-PCR

Total RNA was extracted using the RNeasy plant mini kit (Qiagen), and qRT-PCR was conducted using All-in-One™ qPCR mix (GeneCopoeia) according to Deng *et al.* (2012). The relative expression level for each gene was evaluated using the $\Delta\Delta C_t$ values with *SIActin* as internal control. The primer sequences used are listed in Table S4.

GUS staining

GUS staining was conducted according to Yuan *et al.*, (2019).

Spider mite bioassays

General procedures for treating two-spotted spider mites (*Tetranychus urticae*) were performed according to Li *et al.* (2004). Inoculation assay was done by transferring 15 adult female mites to a single leaf using one-month-old seedlings. Preference assays were performed by placing 10 mites in a 1 cm circle located equidistantly (1 cm) between the single leaflets derived from 5-week-old WT and transgenic plants. Spider mites were counted at 1 h after initiating the trial. Fecundity assays started with transferring five adult female mites to leaf discs (12 mm) of WT and transgenic plants that were placed on wetted cotton (Rodriguez *et al.*, 1971; Rodriguez *et al.*, 1972). Eggs were counted using a microscope at 24-h intervals for four days.

RNA-Seq analysis

RNA-Seq was conducted by Shanghai Majorbio Biopharm Technology Co., Ltd. Total RNA of the leaf tissue was isolated with the DNeasy plant mini kit (Qiagen). RNA-Seq was performed according to conditions as previously reported (Zhang *et al.*, 2015).

Promoter analysis and dual-luciferase transient expression assay

Motif promoter sequences were analysed using PLACE Signal Scan search software (<http://www.dna.affrc.go.jp/PLACE/signalscan.html>). Dual-luciferase transient expression assay was performed by amplifying and cloning the sequence of gene-coding regions into the pGreenII 62-SK vector (Hellens *et al.*, 2005). GAL4 sequence or gene promoter sequences were cloned into pGreenII 0800-LUC vector (Hellens *et al.*, 2005). The activities of LUC and REN luciferases were measured by Luminoskan Ascent microplate luminometer using a dual-luciferase assay kit (Promega, Madison, WI, USA). Six biological repeats were used for each pair of vectors. All primers for this assay are listed in Table S4.

Protein expression and EMSA

Truncated gene-coding regions were cloned into pGEX-4T-1 bacterial expression vectors (GE Healthcare Life Science, China) and expressed in *Escherichia coli* strain BM Rosetta (DE3). Recombinant proteins were induced with 0.5 mM isopropyl-β-D-thiogalactopyranoside for 16 h at 28 °C and purified through a GST-tagged protein purification kit (Clontech, Palo Alto, CA, USA). LightShift chemiluminescent EMSA kit (Thermo Fisher Scientific, Rockford, IL, USA) was used according to Han *et al.* (2016). EMSA assay was conducted according to Yuan *et al.*, (2019). All primers designed for EMSA are listed in Table S4.

ChIP-qPCR assay

ChIP-qPCR assay was conducted as described by Qin *et al.* (2012). All primers designed for ChIP-qPCR analysis are shown in Table S4.

Statistics

Unpaired, two-tailed Student's *t*-tests were performed to compare individual lines with their relevant controls. Univariate ANOVA followed by the post hoc Tukey test of multiple pairwise comparisons was used for the comparison among the measurements of multiple experiment designs. $P < 0.05$ was considered a significant difference, and $P < 0.01$ was considered a highly significant difference.

Acknowledgements

This work was supported by National Key R&D Program of China (2016YFD0400100) and National Natural Science Foundation of China (31272165). We greatly appreciate Prof. Jianye Chen and Prof. Jianfei Kuang for providing experimental instruction. We greatly appreciate Prof. Mondher Bouzayen and Dr. Mohamed Zouine for providing seeds of P-*SIARF4*-GUS and *Slarf4* CRISPR-Cas9 tomato plants.

Conflicts of interest statement

The authors declare no conflicts of interest.

Author contributions

W.D. and Z.G.L. conceived the research. Y.J.Y., X.X., Y.Q.L., Z.H.G., X.W.H., M.B.W., Y.D.L., F.Y., X.L.Z., W.F.Z., Y.W.T. and B.H.F. performed experiments. W.F.Z. analysed the data. W.D. and Y.J.Y. wrote the manuscript. C.Z.J. revised the manuscript.

References

- Chang, J., Yu, T., Yang, Q., Li, C., Xiong, C., Gao, S., Xie, Q. *et al.* (2018) Hair, encoding a single C2H2 zinc-finger protein, regulates multicellular trichome formation in tomato. *Plant J.* **96**, 90–102.
- Ckurshumova, W., Smirnova, T., Marcos, D., Zayed, Y. and Berleth, T. (2014) Irrepressible MONOPTEROS/ARF5 promotes de novo shoot formation. *New Phytol.* **204**, 556–566.
- Deng, W., Yang, Y., Ren, Z., Audran-Delalande, C., Mila, I., Wang, X., Song, H. *et al.* (2012) The tomato *SlAA15* is involved in trichome formation and axillary shoot development. *New Phytol.* **194**, 379–390.
- Dermauw, W., Wybouw, N., Rombauts, S., Menten, B., Vontas, J., Grbić, M., Clark, R.M. *et al.* (2013) A link between host plant adaptation and pesticide resistance in the polyphagous spider mite *Tetranychus urticae*. *Proc. Natl. Acad. Sci. USA*, **110**, 113–122.
- Fobert, P.R., Coen, E.S., Murphy, G.J. and Doonan, J.H. (1994) Patterns of cell division revealed by transcriptional regulation of genes during the cell cycle in plants. *EMBO J.* **13**, 616–624.
- Gao, S., Gao, Y., Xiong, C., Yu, G., Chang, J., Yang, Q., Yang, C. *et al.* (2017) The tomato B-type cyclin gene, *SlCycB2*, plays key roles in reproductive organ development, trichome initiation, terpenoids biosynthesis and *Prodenia litura* defense. *Plant Sci.* **262**, 103–114.
- Glas, J.J., Schimmel, B.C., Alba, J.M., Escobar-Bravo, R., Schuurink, R.C. and Kant, M.R. (2012) Plant glandular trichomes as targets for breeding or engineering of resistance to herbivores. *Int. J. Mol. Sci.* **13**, 17077–17103.
- Glover, B.J., Perez-Rodriguez, M. and Martin, C. (1998) Development of several epidermal cell types can be specified by the same MYB-related plant transcription factor. *Development*, **125**, 3497–3508.
- Guilfoyle, T.J. and Hagen, G. (2012) Getting a grasp on domain III/IV responsible for Auxin Response Factor–IAA protein interactions. *Plant Sci.* **190**, 82–88.
- Hamza, R., Pérez-Hedo, M., Urbaneja, A., Rambla, J.L., Granell, A., Gaddour, K., Beltrán, J.P. *et al.* (2018) Expression of two barley proteinase inhibitors in tomato promotes endogenous defensive response and enhances resistance to *Tuta absoluta*. *BMC Plant Biol.* **18**, 24.
- Han, Y.C., Kuang, J.F., Chen, J.Y., Liu, X.C., Xiao, Y.Y., Fu, C.C., Wang, J.N. *et al.* (2016) Banana transcription factor MaERF11 recruits histone deacetylase MaHDA1 and represses the expression of MaACO1 and expansins during fruit ripening. *Plant Physiol.* **171**, 1070–1084.
- Handley, R., Ekblom, B. and Ågren, J. (2005) Variation in trichome density and resistance against a specialist insect herbivore in natural populations of *Arabidopsis thaliana*. *Ecol. Entomol.* **30**, 284–292.
- Hellens, R.P., Allan, A.C., Friel, E.N., Bolitho, K., Grafton, K., Templeton, M.D., Karunairetnam, S. *et al.* (2005) Transient expression vectors for functional genomics, quantification of promoter activity and RNA silencing in plants. *Plant Methods*, **1**, 13.
- Hirt, H., Mink, M., Pfosser, M., Bögre, L., Györgyey, J., Jonak, C., Gartner, A. *et al.* (1992) Alfalfa cyclins: differential expression during the cell cycle and in plant organs. *Plant Cell*, **4**, 1531–1538.
- Horgan, F.G., Quiring, D.T., Lagnaoui, A. and Pelletier, Y. (2009) Effects of altitude of origin on trichome-mediated anti-herbivore resistance in wild Andean potatoes. *Flora*, **204**, 49–62.
- Ishida, T., Kurata, T., Okada, K. and Wada, T. (2008) A genetic regulatory network in the development of trichomes and root hairs. *Annu. Rev. Plant Biol.* **59**, 365–86.
- Johnson, R. (1992) Past, Present and future opportunities in breeding for disease resistance. *Euphytica*, **63**, 3–22.
- Krogan, N.T. and Berleth, T. (2012) A dominant mutation reveals asymmetry in MP/ARF5 function along the adaxial-abaxial axis of shoot lateral organs. *Plant Signal Behav.* **7**, 940–943.
- Li, L., Zhao, Y., McCaig, B.C., Wingerd, B.A., Wang, J., Whalon, M.E., Pichersky, E. *et al.* (2004) The tomato homolog of CORONATINE-INSENSITIVE1 is required for the maternal control of seed maturation, jasmonate-signaled defense responses, and glandular trichome development. *Plant Cell*, **16**, 126–143.
- Li, Z., Peng, R., Tian, Y., Han, H., Xu, J. and Yao, Q. (2016) Genome-Wide identification and analysis of the MYB transcription factor superfamily in *Solanum lycopersicum*. *J. Plant Cell Physiol.* **56**, 1657–1677.
- Lovelli, S., Scopa, A., Perniola, M., Tommaso, T. and Sofo, A. (2012) Abscisic acid root and leaf concentration in relation to biomass partitioning in salinized tomato plants. *J. Plant Physiol.* **169**, 226–233.
- Machado, A., Wu, Y., Yang, Y., Llewellyn, D.J. and Dennis, E.S. (2009) The MYB transcription factor GhMYB25 regulates early fibre and trichome development. *Plant J.* **59**, 52–62.
- Maes, L. and Goossens, A. (2010) Hormone-mediated promotion of trichome initiation in plants is conserved but utilizes species and trichome-specific regulatory mechanisms. *Plant Signal Behav.* **5**, 205–207.
- Meijer, M. and Murray, J.A. (2001) Cell cycle controls and the development of plant form. *Curr. Opin. Plant Biol.* **4**, 44–49.
- Morohashi, K. and Grotewold, E. (2009) A systems approach reveals regulatory circuitry for Arabidopsis trichome initiation by the GL3 and GL1 selectors. *PLoS Genet.* **5**, e1000396.
- Payne, T., Clement, J., Arnold, D. and Lloyd, A. (1999) Heterologous myb genes distinct from *GL1* enhance trichome production when overexpressed in *Nicotiana tabacum*. *Development*, **126**, 671–682.
- Qin, G., Wang, Y., Cao, B., Wang, W. and Tian, S. (2012) Unraveling the regulatory network of the MADS box transcription factor RIN in fruit ripening. *Plant J.* **70**, 243–255.
- Ren, Z., Li, Z., Miao, Q., Yang, Y., Deng, W. and Hao, Y. (2011) The auxin receptor homologue in *Solanum lycopersicum* stimulates tomato fruit set and leaf morphogenesis. *J. Exp. Bot.* **62**, 2815–2826.
- Rodriguez, J.G., Dabrowski, Z.T., Stoltz, L.P., Chaplin, C.E. and Smith, W.O. (1971) Studies on resistance of strawberries to mites. 2. Preference and nonpreference responses of *Tetranychus urticae* and *T. turestani* to water-soluble extracts of foliage. *J. Econ. Entomol.* **64**, 383–386.
- Rodriguez, J.G., Knavel, D.E. and Aina, O.J. (1972) Studies in the resistance of tomatoes to mites. *J. Econ. Entomol.* **65**, 50–53.
- Sagar, M., Chervin, C., Mila, I., Hao, Y., Roustan, J.P., Benichou, M., Gibon, Y. *et al.* (2013) *SIARF4*, an auxin response factor involved in the control of sugar metabolism during tomato fruit development. *Plant Physiol.* **161**, 1362–1374.
- Schillmiller, A., Shi, F., Kim, J., Charbonneau, A.L., Holmes, D., Daniel Jones, A. and Last, R.L. (2010) Mass spectrometry screening reveals widespread diversity in trichome specialized metabolites of tomato chromosomal substitution lines. *Plant J.* **62**, 391–403.
- Schnittger, A., Schöbinger, U., Stierhof, Y.D. and Hülskamp, M. (2002) Ectopic B-type cyclin expression induces mitotic cycles in endoreduplicating Arabidopsis trichomes. *Curr. Biol.* **12**, 415–420.
- Szemenyei, H., Hannon, M. and Long, J.A. (2008) TOPLESS mediates auxin-dependent transcriptional repression during Arabidopsis embryogenesis. *Science*, **319**, 1384–1386.

- Turlings, T.C., Loughrin, J.H., McCall, P.J., R6se, U.S., Lewis, W.J. and Tumlinson, J.H. (1995) How caterpillar-damaged plants protect themselves by attracting parasitic wasps. *Proc. Natl. Acad. Sci. USA*, **92**, 4169–4174.
- Van Leeuwen, T., Stillatus, V. and Tirry, L. (2004) Genetic analysis and cross-resistance spectrum of a laboratory-selected chlorfenapyr resistant strain of two-spotted spider mite (Acari: Tetranychidae). *Exp. Appl. Acarol.* **32**, 249.
- Wang, R. and Estelle, M. (2014) Diversity and specificity: auxin perception and signaling through the TIR1/AFB pathway. *Curr. Opin. Plant Biol.* **21**, 51–58.
- Wang, S., Wang, J.W., Yu, N., Li, C.H., Luo, B., Gou, J.Y., Wang, L.J. et al. (2004) Control of plant trichome development by a cotton fiber MYB gene. *Plant Cell*, **16**, 2323–2334.
- Wang, S., Kwak, S.H., Zeng, Q., Ellis, B.E., Chen, X.Y., Schiefelbein, J. and Chen, J.G. (2007) TRICHOMELESS1 regulates trichome patterning by suppressing *GLABRA1* in *Arabidopsis*. *Development*, **134**, 3873–3882.
- Xu, J., van Herwijnen, Z.O., Dr6ger, D.B., Sui, C., Haring, M.A. and Schuurink, R.C. (2018) SIMYC1 regulates VI type glandular trichome formation and terpene biosynthesis in tomato glandular cells. *Plant Cell*, **30**, 2988–3005.
- Yang, C. and Ye, Z. (2013) Trichomes as models for studying plant cell differentiation. *Cell Mol. Life Sci.* **70**, 1937–1948.
- Yang, C., Li, H., Zhang, J., Luo, Z., Gong, P., Zhang, C., Li, J. et al. (2011) A regulatory gene induces trichome formation and embryo lethality in tomato. *Proc. Natl. Acad. Sci. USA*, **108**, 11836–11841.
- Yang, C., Gao, Y., Gao, S., Yu, G., Xiong, C., Chang, J., Li, H. et al. (2015) Transcriptome profile analysis of cell proliferation molecular processes during multicellular trichome formation induced by tomato *Wo v* gene in tobacco. *BMC Genom.* **16**, 868.
- Yuan, Y., Xu, X., Gong, Z., Tang, Y., Wu, M., Yan, F., Zhang, X. et al. (2019) Auxin response factor 6A regulates photosynthesis, sugar accumulation, and fruit development in tomato. *Horticulture Res.* **6**, 85.
- Zhang, X., Yan, F., Tang, Y., Yuan, Y., Deng, W. and Li, Z. (2015) Auxin response gene *SIARF3* plays multiple roles in tomato development and is involved in the formation of epidermal cells and trichomes. *Plant Cell Physiol.* **56**, 2110–2124.
- Zhao, P., Li, Q., Li, J. and Wang, L. (2014) Genome-wide identification and characterization of R2R3MYB family in *Solanum lycopersicum*. *Mol. Genet. Genom.* **289**, 1183–1207.
- Zouine, M., Fu, Y., Chateigner-Boutin, A.L., Mila, I., Frasse, P., Wang, H., Audran, C. et al. (2014) Characterization of the tomato ARF gene family uncovers a multi-levels post-transcriptional regulation including alternative splicing. *PLoS One*, **9**, e84203.

Supporting information

Additional supporting information may be found online in the Supporting Information section at the end of the article.

- Figure S1** Density analysis of epidermal pavement cells in the leaves of IAA-treated tomato plants.
- Figure S2** qRT-PCR analysis of *SIARF4* expression levels
- Figure S3** Density analysis of epidermal pavement cells in the leaves of OE-*SIARF4* and RNAi-*SIARF4* plants.
- Figure S4** Trichomes densities of fruits in *SIARF4* transgenic plants.

Figure S5 Trichomes densities of leaves in *Slarf4* CRISPR-Cas9 mutants.

Figure S6 RNA-Seq analysis of RNAi-*SIARF4* plants.

Figure S7 RNA-Seq analysis of RNAi-*SIARF4* plants.

Figure S8 SDS-PAGE gel stained with Coomassie brilliant blue demonstrating the affinity purification of recombinant GST-tSIARF4 protein used for EMSA.

Figure S9 qRT-PCR analysis of the expression levels of *SITHM1* and *SIMYB52* genes in RNAi-*SIARF4* and OE-*SIARF4* plants.

Figure S10 Sequence alignments of *SIMYB52* and *SITHM1* with known proteins from the same subgroup

Figure S11 Phylogenetic trees of *SITHM1* and *SIMYB52* with homologous proteins from other species

Figure S12 qRT-PCR analysis of *SITHM1* expression levels.

Figure S13 Diagrams of the reporter and effector vectors and transcriptional activation activity assay of *SITHM1*

Figure S14 Density of epidermal pavement cells in RNAi-*SITHM1* plants

Figure S15 qRT-PCR analysis of *SIMYB52* expression levels.

Figure S16 Density of epidermal pavement cells in RNAi-*SIMYB52* plants.

Figure S17 Spider mite bioassay of *SIMYB52* RNAi plants

Figure S18 qRT-PCR analysis of the expression of *SICyCB2* in leaves of *SITHM1* and *SIMYB52* transgenic lines.

Figure S19. SDS-PAGE gel stained with coomassie brilliant blue demonstrating affinity purification of the recombinant GST-tSIARF4 and GST-tMYB52 used for the EMSA assay

Figure S20 Agricultural trait analysis of the *SIARF4* transgenic plants.

Figure S21 Agricultural trait analysis of the *SITHM1* transgenic plants.

Figure S22 Agricultural trait analysis of the *SIMYB52* transgenic plants.

Figure S23 Expression patterns of *SIARF3*, *SIARF4*, *SITHM1*, *SIMYB52* and *SICyCB2* genes in response to IAA treatments

Figure S24 Expression patterns of *SIARF3*, *SIARF4*, *SITHM1*, *SIMYB52* and *SICyCB2* genes in response to JA treatments.

Figure S25 qRT-PCR analysis of the expression of *SIARF3* in leaves of *SIARF4* transgenic lines

Figure S26 Density analysis of II, V and VI type trichomes of RNAi-*SIARF3* and RNAi-*SIARF4* crossed plants.

Figure S27 Number of trichomes per epidermal cell of RNAi-*SIARF3* and RNAi-*SIARF4* crossed plants.

Figure S28 Density of epidermal pavement cells of RNAi-*SIARF3* and RNAi-*SIARF4* crossed plants.

Table S1 All DEGs in RNAi-*SIARF4* plants

Table S2 GO function and pathway enrichment analyses of DEGs in RNAi-*SIARF4* plants

Table S3 DEGs encoding TFs in RNAi-*SIARF4* plants.

Table S4 Primers used in this study.